Journal of Solid State Chemistry 183 (2010) 2268–2273

Contents lists available at ScienceDirect

Journal of Solid State Chemistry

journal homepage: www.elsevier.com/locate/jssc

Thermal annealing synthesis of titanium-dioxide nanowire–nanoparticle hetero-structures

Choongho Yu [a,b,*], Jongbok Park [a]

[a] Department of Mechanical Engineering, Texas A&M University, College Station, TX 77843, USA
[b] Materials Science and Engineering Program, Texas A&M University, College Station, TX 77843, USA

ARTICLE INFO

Article history:
Received 7 June 2010
Received in revised form
10 August 2010
Accepted 16 August 2010
Available online 20 August 2010

Keywords:
Thermal annealing synthesis
Titanium-dioxide
TiO_2
Hetero-structure
Nanowire
Nanoparticle
Dye-sensitized solar cell

ABSTRACT

Crystalline TiO_2 nanowire–nanoparticle hetero-structures were successfully synthesized from titanium foils by using a simple thermal annealing method with the aid of $CuCl_2$ at the atmospheric pressure. Nanowires were grown from Ti foils by simply annealing Ti foils at 850 °C. Then, $TiCl_4$ was delivered to TiO_2 nanowires so as to precipitate TiO_2 nanoparticles on nanowire surfaces. At 750 °C reaction temperature, nanoparticles of tens of nanometers in diameter were well distributed on pre-grown nanowire forests. Nanoparticles were likely to be precipitated by $TiCl_4$ decomposition or oxidation and that require high temperatures above ~650 °C. Electron microscopy, X-ray diffraction, and UV–vis spectroscopy analyses show they have the rutile polycrystalline structure with a slightly enlarged bandgap compared to that of bulk TiO_2. The influence of key synthesis parameters including reaction temperature, reaction time, and quantity of supplied materials on the incorporating nanoparticles was also systematically studied. The optimum reaction condition in the present paper was identified to be 750 °C annealing with repetitive 20 min reactions. A higher reaction temperature yielded larger diameter particles, and higher loading of Ti produced dense particles without changing the particle size. Finally, this method could be utilized for synthesizing other metal oxide nanowires–nanoparticle hetero-structures.

1. Introduction

Titanium dioxide is one of the most popular oxide materials due to their superior characteristics in various applications including photoelectrochemistry. Particularly, nanostructured TiO_2 have recently been of great interest because nanostructures often improve photocatalytic performance and/or exhibit properties different from bulk counterparts. For example, porous films made of TiO_2 nanoparticles are used for dye-sensitized solar cells (DSSC) [1,2] due to enlarged surface areas for dye absorption. However, the speed of electron diffusion across nanoparticle junctions is several orders of magnitude smaller than that of bulk crystalline TiO_2 due to frequent electron trapping at the junctions of nanoparticles [3–8]. In this case, separated charges are recombined before they reach electrodes. One-dimensional TiO_2 nanostructures such as nanowires and nanotubes have been suggested to eliminate such problems [9,10]. Nanowires can be grown from electrodes, providing a pathway of transporting charges without grain boundaries and junctions. Once electrons are injected to the conduction band of TiO_2, recombination can be minimized due to their relatively wide band gap. Another advantage of one-dimensional nanostructures is the ability to capture scattered light in the cell, which is possible to augment light harvesting [11]. Nevertheless, the surface area required for dye absorption in one-dimensional structures is not as large as that of porous nanoparticle films. In this regard, nanoparticle–nanowire hetero-structure may be able to maximize both dye absorption and charge transport. In addition, similar methodologies for enlarging surface areas of nanostructured metal oxides could be utilized for other applications including sensors [12] and water splitting [13].

Various methods have been reported to synthesize either nanowires or nanoparticles including hydrothermal [14,15], hydrolysis [16], titanium anodization [17], template synthesis methods using porous membranes [18], sol–gel methods [19], and thermal annealing [20]. These methods typically produce one of the following structures—amorphous, brookite, anatase, rutile TiO_2, or TiO_2-B. Further thermal annealing processes are typically required for converting amorphous and TiO_2-B structures into crystalline anatase or rutile structures. When nanowires and nanoparticles are separately synthesized and then simply mixed together [11,21], nanowires are not directly connected to

* Corresponding author at: Department of Mechanical Engineering, Materials Science and Engineering Program, Texas A&M University, College station, TX 77843, USA.
E-mail address: chyu@tamu.edu (C. Yu).

0022-4596/$ - see front matter © 2010 Elsevier Inc. All rights reserved.
doi:10.1016/j.jssc.2010.08.022

electrodes, which makes it difficult to avoid charge recombination and improve charge transport. Here, this paper reports a synthesis method to obtain nanowire–nanoparticle tree-like hetero-structures grown from substrates. Nanowires were grown from substrates by a simple annealing method and then nanoparticles were subsequently incorporated into the nanowires. Seven different growth conditions by changing temperatures, times, and Ti quantity revealed reaction mechanisms and optimum conditions. This process requires only simple annealing in a tube furnace with the aid of $CuCl_2$. $TiCl_4$ gas generated from a mixture of Ti/$CuCl_2 \cdot 2H_2O$ was delivered to TiO_2 nanowires by Ar gas, and then it was precipitated into TiO_2 nanoparticles on nanowire surfaces. At 750 °C reaction temperature, nanoparticles of tens of nanometers in diameter were well distributed on pre-grown nanowire forests. Electron microscopy and X-ray diffraction analyses were performed to characterize their structures and UV–vis spectroscopy results are also presented.

2. Experimental details

Nanowire–nanoparticle hetero-structures were synthesized by using the following two-step process. The first step is to grow nanowires whose length and diameter (or width) can be controlled, and the second is to incorporate various size and density nanoparticles into the nanowires. For the nanowire synthesis [20], titanium foils (Sigma-Aldrich, purity 99.7%) were diced into pieces ($\sim$0.5 cm × 0.5 cm × 0.1 mm), and then ultrasonically cleaned in acetone, isopropanol, and deionized (DI) water. Then, a solution of 0.005 M $CuCl_2 \cdot 2H_2O$ (Acros Organics, purity 99%) in DI water was spin-coated three times at 1500 rpm for 20 s, which uniformly distributes $CuCl_2$ on the foil surface. The foil was placed in a covered boat (3 in. long) that maintains $TiCl_4$ gases from being lost to Ar flow easily. Note that 99.999% pure Ar gas was used for all experiments presented in this paper. The boat was inserted to the center of a quartz tube of $\sim$2.3 cm in inner diameter and $\sim$120 cm in length. Prior to heating the tube furnace, $\sim$100 sccm Ar was flowed for 3 min, and then the furnace was heated up to 850 °C with a ramping time of 20 min and an annealing time of 30 min at a continuous $\sim$40 sccm Ar flow throughout the entire synthesis process. Upon heating, $CuCl_2$ decomposes into CuCl and gas-phase Cl_2 above 493 °C [22].

$$CuCl_2(s) \rightarrow CuCl(s/l) + 0.5Cl_2(g) \quad (1)$$

CuCl reacts with Ti even above $\sim$250 °C, remaining solid Cu on the substrate [23,24].

$$Ti(s) + 4CuCl(s) \rightarrow TiCl_4(g) + 4Cu(s) \quad (2)$$

The precipitated Cu on the Ti substrate becomes Ti–Cu eutectic mixture at $\sim$870 °C [25,26], serving as seeds for growing TiO_2 nanowires at a temperature lower than the Ti melting point (1668 °C). Oxygen in the Ar flow or oxygen residues in the reaction tube would have been consumed to form crystalline titanium oxides due to the strong affinity of Ti to oxygen. After synthesizing nanowires, a mixture of titanium (Acros Organics, 100 mesh, purity 99.7%) and $CuCl_2 \cdot 2H_2O$ powders as well as the as-grown TiO_2 nanostructure sample were loaded in a boat. The sample was placed at a downstream 5–6 cm apart from the powder mixture. At room temperature, $\sim$40 sccm Ar was flowed for 2 min in order to purge air in the tube. The furnace was heated without the quartz tube up to a target temperature, 850, 750, or 650 °C, as listed in Table 1. Subsequently, the tube was placed in the furnace with a continuous $\sim$40 sccm Ar flow for 60, 30, or 20 min. The temperature of the sample is expected to be $\sim$1% lower than that of the powder [27]. Heated $CuCl_2$ in the mixed powders decomposes into CuCl, reacting with Ti to produce gas-phase $TiCl_4$. The covered boat has an inlet and outlet so that the Ar flow delivers $TiCl_4$ to the TiO_2 nanowires. Note that the boiling point of $TiCl_4$ is $\sim$136 °C [28]. Then, oxygen and/or water vapor from Ar gas, $CuCl_2 \cdot 2H_2O$ powder, and oxygen residues in the tube convert $TiCl_4$ into TiO_2 by the following reactions [29–31]:

$$TiCl_4(g) + O_2(g) \rightarrow TiO_2(s) + 2Cl_2(g) \quad (3)$$

$$TiCl_4(g) + 2H_2O(g) \rightarrow TiO_2(s) + 4HCl(g) \quad (4)$$

In addition, $TiCl_4$ can also be decomposed by the following reaction. Then, the decomposed titanium can be oxidized on the nanowires as follows:

$$TiCl_4(g) \rightarrow Ti(s) + 2Cl_2(g); \quad Ti(s) + O_2(g) \rightarrow TiO_2(s) \quad (5)$$

These reactions would have also played a role in growing nanowires.

After the reaction, the tube was removed from the furnace and cooled to room temperature. For fast heating and cooling, the quartz tube was connected by flexible tubing so that the tube can be freely placed in and out of the furnace. The same process was repeated twice or three times so as to precipitate TiO_2 nanoparticles on nanowires. At the beginning of each cycle, the mixed powders of Ti and $CuCl_2 \cdot 2H_2O$ was freshly loaded. For uniform nanoparticle distributions, the sample was rotated by 90° for every repetition process.

Seven-different nanoparticle synthesis conditions were carried out as listed in Table 1 for elucidating the influence of three important incorporating parameters reaction temperature, the repetition time, and the amount of mixed powders. Three different annealing temperatures (650, 750, and 850 °C) and three different repetition times (20, 30, and 60 min) were employed in order to identify changes in the size and the density of nanoparticles. In order to keep the temperature for designated time periods in the condition table, the quartz tube was pulled out of the furnace and cooled to room temperature right after each heating process. We also tried to synthesize nanowires and

Table 1
Seven different conditions for synthesizing TiO_2 nanowire–nanoparticle hetero-structures. One parameter was changed at a time in order to identify the influence of each parameter on the growth of the hetero-structures.

Synthesis condition	Nanoparticle growth temperature (°C)	Repetition time (min)	Mixed powders (Ti/$CuCl_2 \cdot 2H_2O$) (g)	Initial wire growth temp./time (°C/min)	Remarks
1	850	60/30/30	0.024/0.086	850/30	
2	750	60/30/30	0.024/0.086	750/30	
3	750	20/20/20/20	0.024/0.086	850/30	
4	750	20/20/20/20	0.012/0.043	850/30	
5	650	20/20/20/20	0.012/0.043	850/30	
6	850	30/20/20/20	0.024/0.086	–	Simultaneous process
7	750	30/20/20/20	0.024/0.086	–	Simultaneous process

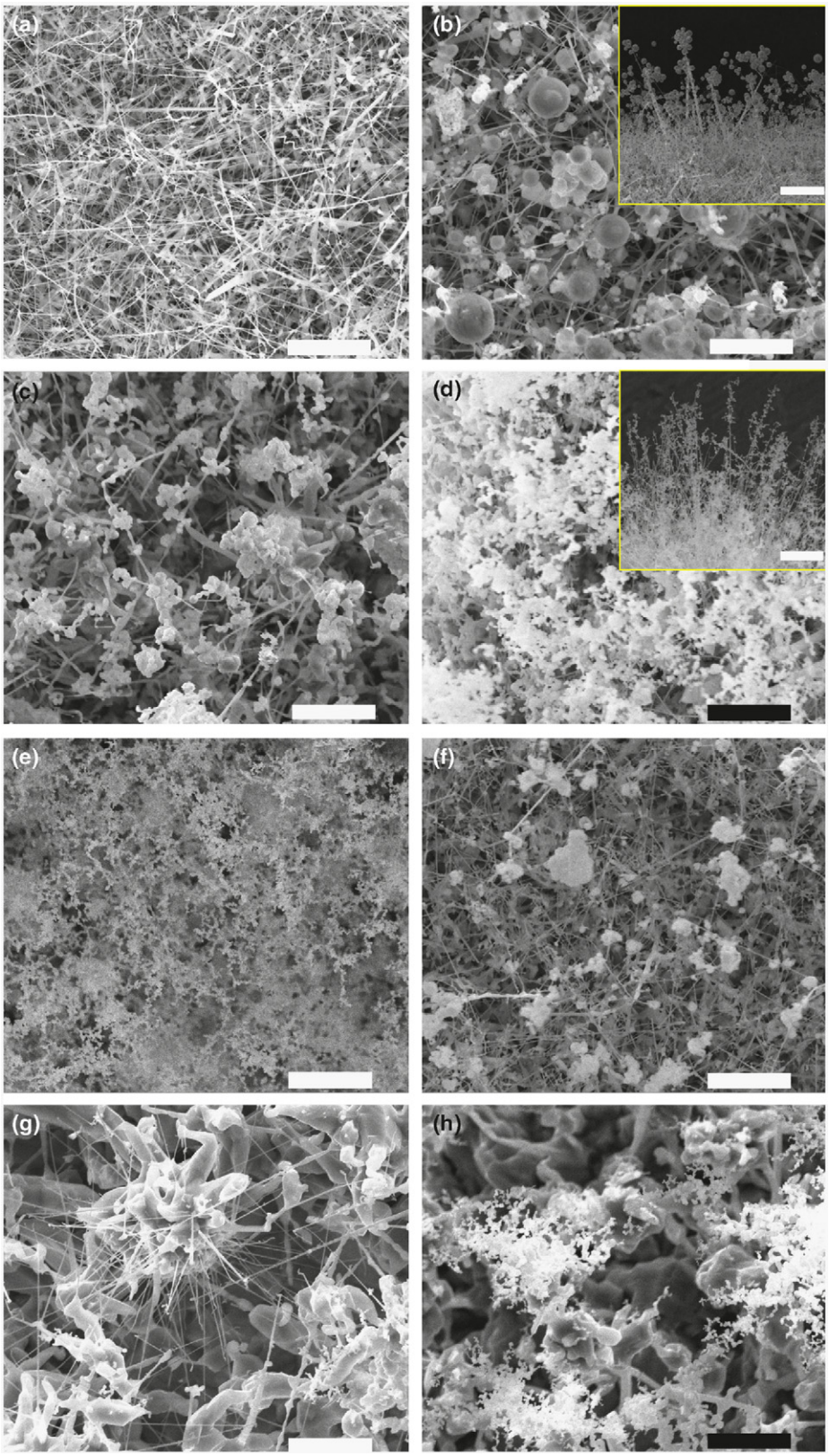

Fig. 1. (a) TiO_2 nanowires grown at an annealing temperature of 850 °C for 30 min. TiO_2 nanowire–nanoparticle hetero-structures grown by using growth conditions listed in Table 1. (b) 60/30/30 min annealing at 850 °C (Condition 1). (c) 60/30/30 min annealing at 750 °C (Condition 2). (d) 20/20/20/20 min annealing at 750 °C (Condition 3). (e) 20/20/20/20 min annealing at 750 °C with a reduced amount of powders (Condition 4). (f) 20/20/20/20 min annealing at 650 °C (Condition 5). (g) 30/20/20/20 min annealing at 850 °C without prior nanowire synthesis processes (Condition 6). (h) 30/20/20/20 min annealing at 750 °C without prior nanowire synthesis processes (Condition 7). The scale bars represent 5 μm except for those in the insets (20 μm).

nanoparticles simultaneously with Conditions 6 and 7. First, the $CuCl_2$ solution was spin-coated on bare Ti foils. Then, both the sample and the Ti/Cu powders were placed together in the tube furnace. The powder mixture was placed at an upstream that was 5–6 cm apart from the Ti foil. Typical conditions for growing nanowires and nanoparticles (30/20/20/20 min repetitive annealing processes at 750 or 850 °C) were used.

The structure, composition, and optical properties of the samples were analyzed by using an X-ray diffractometer (Bruker-AXS D8 VARIO), a field emission scanning electron microscope (FE-SEM, FEI Quanta 600), a transmission electron microscope (TEM, JEOL JEM-2010), and a UV–vis spectroscopy (Hitachi U-4100) with samples prepared by using the synthesis condition 4 in Table 1. For the X-ray diffraction (XRD) analysis, the sample was scanned from $2\theta=20^\circ$ to 60° with a step size and dwell time of 0.01° and 0.1 s, respectively. For the TEM analysis, nanostructures were detached by sonication in deionized water, and then they were dispersed on a thin pure formvar resin coated meshed grids.

3. Results and discussion

The first step, an annealing process of Ti foils at 850 °C for 30 min yielded wire-like slender TiO_2, as shown in Fig. 1(a). Then, the nanowire sample was placed in the tube furnace for incorporating nanoparticles. Nanoparticle synthesis conditions were varied one at a time in order to identify the influence of each parameter on nanoparticle growth. When the reaction time was relatively long (60/30/30 min, Conditions 1 and 2), micron-size particles were precipitated (Fig. 1(b) and (c)). The inset images show particles were attached even on the tip of the wires, suggesting Ti delivered by $TiCl_4$ gas was nucleated into TiO_2 particles. Higher temperature reaction (850 °C, Condition 1) yielded larger particles than 750 °C reaction (Condition 2). In addition, the density of nanowires was decreased due to the relatively long reaction time at high temperatures.

The influence of reaction time on the nanoparticle growth was examined by changing it to 20 min (Conditions 3, 4, and 5). The shorter annealing time reduced particle sizes and maintained the density of nanowires after reactions, as shown in Fig. 1(d) and (e). For Condition 4 (Fig. 1(e)), the amount of the Ti/$CuCl_2\cdot 2H_2O$ mixed powder was reduced to a half from that of Condition 3 (Fig. 1(d)). The size of particles was similar, but higher Ti loading resulted in higher particle density. The particle size appears to be a strong function of the growth temperature, and the particle density depends on the amount of $TiCl_4$ gas. The micrographs show that the particles provide surface areas at least five times larger than those of nanowires only.

In order to further investigate the temperature effect, particle reaction temperature was lowered to 650 °C (Condition 5) from the reaction parameters in Condition 4. The reaction temperature, 650 °C is high enough to generate $TiCl_4$ gas, but particle density in Fig. 1(f) is much lower than particles obtained from Conditions 3 and 4 (Fig. 1(d) and (e)). This result implies that the particle synthesis is dominated by reactions (3) and (5) because hydrolysis of $TiCl_4$ [32], (the reaction (4)) occurs even at temperatures much lower than 650 °C. On the other hand, the initiation of $TiCl_4$ oxidation needs ~830 °C [29], and the decomposition of $TiCl_4$ occurs above 650 °C [30]. Decomposed titanium can be readily oxidized at high temperatures like 750 and 850 °C. Particle sizes on the sample grown at 850 °C (Fig. 1(b)) were larger than those of 750 °C (Fig. 1(c)), indicating the reaction (5) (the decomposition and subsequent titanium oxidation) is a dominant reaction for Conditions 3 and 4. At 850 °C, the reaction (3) ($TiCl_4$ oxidation) is likely to participate in producing nanoparticles. Note that oxygen was not supplied externally to the tube furnace during the reaction, but the oxygen is typically present in Ar gas as impurity (oxygen in the 99.999% pure Ar gas is typically less than ~5 ppm). This result suggests that an external supply of oxygen may not be necessary or should be avoided for incorporating TiO_2 nanoparticles. Conditions 6 and 7 (Fig. 1(g) and (h)) were tested for simultaneously synthesizing nanowires and nanoparticles, but they yielded micron-scale structures with a low density of nanowires. The structures synthesized at 850 °C are thicker than those of 750 °C. When wires were growing, $TiCl_4$ gas might have facilitated TiO_2 crystallization in the radial direction as well as in the wire axial direction rather than separated nanoparticle precipitation.

Fig. 2 shows a schematic of the proposed reaction mechanism for synthesizing the hetero-structures. First, nanowires were synthesized and used as reaction sites for precipitating nanoparticles (Fig. 2(a)). Then, $TiCl_4$ gas was delivered to the nanowires by heating Ti/$CuCl_2\cdot 2H_2O$ powders. At temperatures higher than

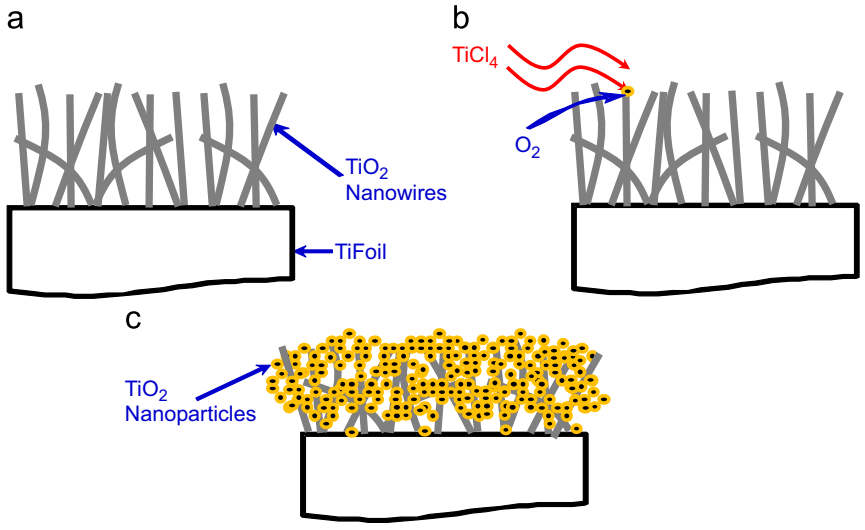

Fig. 2. Schematic of proposed reaction mechanisms for synthesizing the hetero-structures. (a) TiO_2 nanowires were grown as base structures for capturing $TiCl_4$ gas. (b) $TiCl_4$ gas was oxidized, precipitating crystalline TiO_2 nanoparticles. (c) Repeated particle-incorporation process created tree-like hetero-structures. Note that elevated reaction temperatures merged nanowires and nanoparticles as shown in Fig. 3.

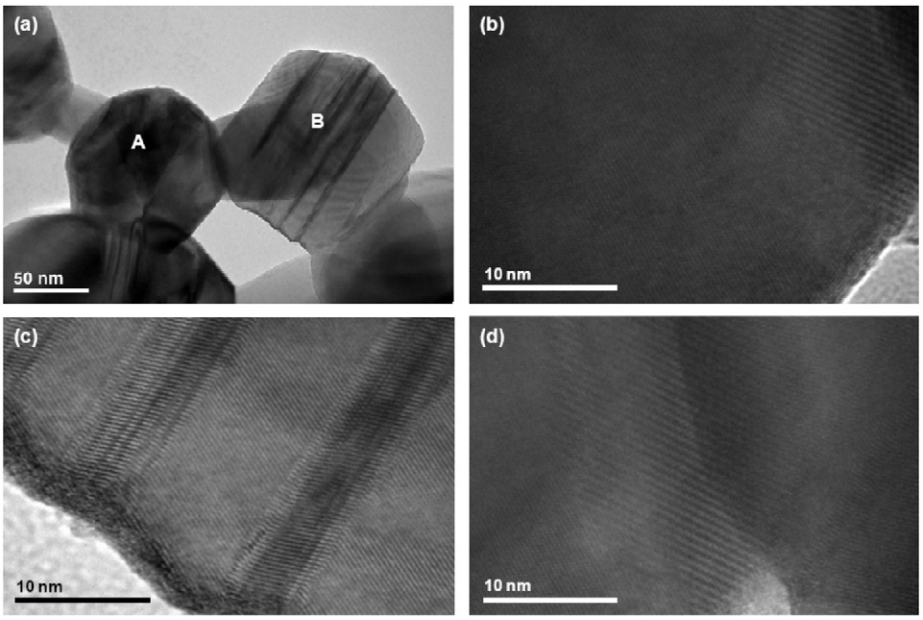

Fig. 3. (a) Nanoparticles and nanowires were joined together, comprising tree-like hetero-structures. (b) A portion of the particle A shows a polycrystalline structure. (c) A portion of the particle B shows twin boundaries. (d) The particles A and B are merged together as evident from the image of the interface. The sample was prepared at 750 °C with 20/20/20/20 min repetition times (Condition 4).

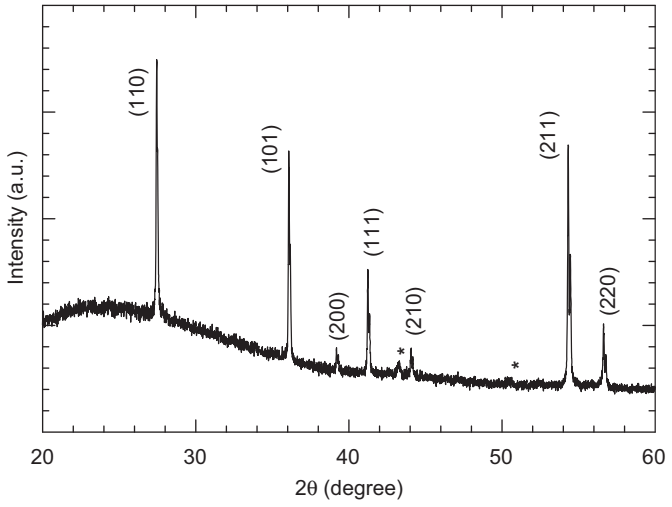

Fig. 4. XRD patterns show the nanowire–nanoparticle hetero-structure has the rutile form of TiO_2. The scanned sample was synthesized at 750 °C with 20/20/20/20 min reaction times for growing nanoparticles (Condition 4). Crystal directions of the rutile structure are designated in the figure. Note that small peaks (*) are likely to be from Cu, which was used for obtaining $TiCl_4$ gas.

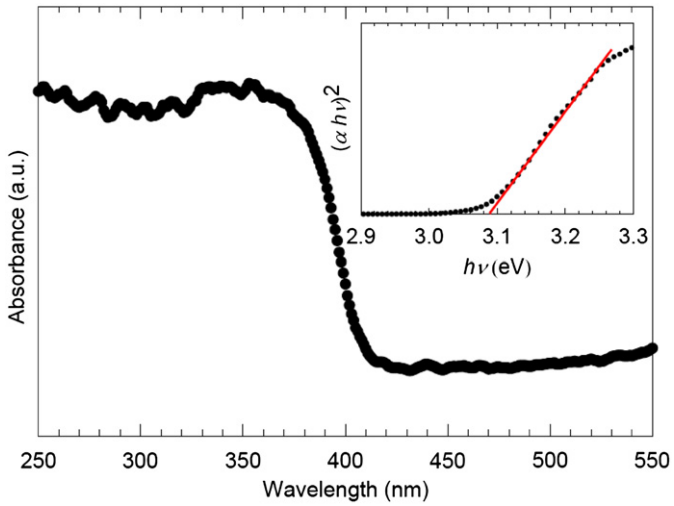

Fig. 5. Absorbance of nanowire–nanoparticle rutile TiO_2 hetero-structures. The inset shows $(\alpha h\nu)^2$ as a function of photon energy ($h\nu$). The crossover point of the slope (indicated by the red line) to the $h\nu$ axis represents the band gap. The scanned sample was synthesized at 750 °C with 20/20/20/20 min reaction times for growing nanoparticles (Condition 4) Fig. 1. (For interpretation of the references to color in this figure legend, the reader is referred to the web version of this article.)

~650 °C, the $TiCl_4$ gas was decomposed into Ti, which was oxidized on TiO_2 nanowire surfaces (Fig. 2(b)). Repeating the particle incorporation process resulted in tree-like hetero-structures shown in Fig. 2(c). Similar processes can be used for growing such hetero-structures with different metal oxides such as copper oxides, zinc oxides, iron oxides, tin oxides, and cobalt oxides, which yield hybrid systems with different band gap materials. Note that metal oxide nanostructures have been synthesized by many different methods [33,34].

TEMs of nanoparticle–nanowire hetero-structures prepared at 750 °C with 20/20/20/20 min repetition times (Condition 4) are shown in Fig. 3. The nanoparticles have polycrystalline structures as evident from the different crystal growth directions in Fig. 3(b,d) (a portion of the particle labeled as A) as well as twin boundaries observed from the particle B (Fig. 3(c)). It is likely that the polycrystalline structure is from the repeated annealing processes. Note that nanowires prior to the nanoparticle incorporation have the single crystalline rutile structure. The interface between the particles labeled as A and B (Fig. 3(d)) shows that particles were merged together.

XRD peaks in Fig. 4 indicate that both nanowires and nanoparticles have the rutile structure, which is typical for TiO_2 synthesized at a temperature higher than ~600 °C [35–38]. The rutile TiO_2 has the primitive tetragonal crystal structure with lattice parameters of $a=0.4593$ and $c=0.2959$ nm (JCPDS file no. 21-1276). Chlorine-containing compounds such as $TiCl_2$, $TiCl_3$,

$TiCl_4$, and $CuTiCl_4$ were not detected. Small additional peaks matched with Cu were found. Cu was used for obtaining $TiCl_4$, and was likely to be delivered to the sample by Ar flow. UV–vis light absorption spectroscopy (UV–vis) analysis was also performed, and absorbance is plotted as a function of photon wavelength as shown in Fig. 5. The absorbance data can be related to the optical band gap by using the following relation [39,40]:

$$\alpha h\nu = C(h\nu - E_g)^n \quad (6)$$

where α, $h\nu$, C, and E_g stand for the absorption coefficient, photon energy, a constant, and the optical bandgap, respectively. For direct and indirect band gaps, n is 0.5 and 2, respectively. When $(\alpha h\nu)^2$ is plotted against $h\nu$, the crossover point of the slope (depicted as a red line in the inset of Fig. 5) to the $h\nu$ axis indicates the band gap. Bulk rutile TiO_2 band gap is 3.02–3.04 eV [40–43], but the sample shows a slightly enlarged gap $\sim$3.09 eV. The broadening of the band gap is often attributed to quantum confinement effects in nanostructured TiO_2 [40,41].

4. Conclusions

Crystalline TiO_2 nanowire–nanoparticle hetero-structures were successfully synthesized from titanium foils by using a simple thermal annealing method at the atmospheric pressure. The synthesis method does not require complicated nor long-time reaction processes, but needs only simple annealing in a tube furnace with the aid of $CuCl_2$ for both nanowire and nanoparticles. Nanowires were grown from Ti foils by simply annealing Ti foil at 850 °C. Then, for incorporating nanoparticles on the nanowires, $TiCl_4$ gas generated from a mixture of $Ti/CuCl_2 \cdot 2H_2O$ powders was delivered to TiO_2 nanowires by Ar gas, which precipitated TiO_2 nanoparticles on nanowire surfaces. At 750 °C reaction temperature, nanoparticles of tens of nanometers in diameter were well distributed on pre-grown nanowire forests. Electron microscopy, X-ray diffraction, and UV–vis spectroscopy analyses show they have the rutile polycrystalline structure with a slightly enlarged bandgap compared to that of bulk TiO_2. The influence of key synthesis parameters – reaction temperature, reaction time, and quantity of supplied materials – on the incorporating nanoparticles was also systematically studied. The optimum reaction condition in the present paper was identified to be at 750 °C annealing with repetitive 20 min reactions. A higher reaction temperature yielded larger diameter particles (up to microns), and higher loading of Ti produced dense particles without changing the particle size. After a low temperature reaction at 650 °C, nanoparticle forests were not observed because nanoparticles were likely to be precipitated by $TiCl_4$ decomposition and oxidation that require high temperatures above $\sim$650 °C. Finally, this method could be utilized for synthesizing other metal oxide nanowires–nanoparticle hetero-structures.

Acknowledgments

The authors gratefully acknowledge financial supports from the US National Science Foundation (Award no. 0854467) and the National Research Foundation of Korea (the Pioneer Research Center Program) funded by the Ministry of Education, Science and Technology (MEST) (Grant no. 2010-0002231), and thank H. Kim's assistance for taking TEMs.

References

[1] B. Oregan, M. Gratzel, Nature 353 (1991) 737.
[2] M. Gratzel, J. Photochem. Photobiol. A 164 (2004) 3.
[3] A. Solbrand, H. Lindstrom, H. Rensmo, A. Hagfeldt, S.-E. Lindquist, S. Sodergren, J. Phys. Chem. B 101 (1997) 2514.
[4] A.C. Fisher, L.M. Peter, E.A. Ponomarev, A.B. Walker, K.G.U. Wijayantha, J. Phys. Chem. B 104 (2000) 949–958.
[5] J. van de Lagemaat, N.-G. Park, A.J. Frank, J. Phys. Chem. B 104 (2000) 2044–2052.
[6] N. Kopidakis, E.A. Schiff, N.-G. Park, J. van de Lagemaat, A.J. Frank, J. Phys. Chem. B 104 (2000) 3930–3936.
[7] N. Kopidakis, N.R. Neale, K. Zhu, J. van de Lagemaat, A.J. Frank, Appl. Phys. Lett. 87 (2005) 202106.
[8] S. Nakade, Y. Saito, W. Kubo, T. Kitamura, Y. Wada, S. Yanagida, J. Phys. Chem. B 107 (2003) 8607.
[9] M. Paulose, K. Shankar, O.K. Varghese, G.K. Mor, B. Hardin, C.A. Grimes, Nanotechnology 17 (2006) 1446.
[10] K. Shankar, G.K. Mor, H.E. Prakasam, S. Yoriya, M. Paulose, O.K. Varghese, C.A. Grimes, Nanotechnology 18 (2007) 11.
[11] B. Tan, Y.Y. Wu, J. Phys. Chem. B 110 (2006) 15932.
[12] C. Yu, Q. Hao, S. Saha, L. Shi, X. Kong, Z.L. Wang, Appl. Phys. Lett. 86 (2005) 063101.
[13] X. Yang, A. Wolcott, G. Wang, A. Sobo, R.C. Fitzmorris, F. Qian, J.Z. Zhang, Y. Li, Nano Lett. 9 (2009) 2331–2336.
[14] C.J. Barbe, F. Arendse, P. Comte, M. Jirousek, F. Lenzmann, V. Shklover, M. Gratzel, J. Am. Ceram. Soc. 80 (1997) 3157–3171.
[15] R. Yoshida, Y. Suzuki, S. Yoshikawa, J. Solid State Chem. 178 (2005) 2179.
[16] A.K. John, G.D. Surender, J. Mater. Sci. 40 (2005) 2999–3001.
[17] M. Paulose, G.K. Mor, O.K. Varghese, K. Shankar, C.A. Grimes, J. Photochem. Photobiol. A 178 (2006) 8.
[18] H. Imai, Y. Takei, K. Shimizu, M. Matsuda, H. Hirashima, J. Mater. Chem. 9 (1999) 2971–2972.
[19] B.B. Lakshmi, P.K. Dorhout, C.R. Martin, Chem. Mater. 9 (1997) 857–862.
[20] J. Park, Y. Ryu, H. Kim, C. Yu, Nanotechnology 10 (2009) 105608.
[21] J.-J. Wu, G.-R. Chen, C.-C. Lu, W.-T. Wu, J.-S. Chen, Nanotechnology 19 (2008) 105702.
[22] M.W. Chase, in: NIST-JANAF Thermochemical Tables, American Chemical Society, Washington, DC, 1998, p. 817.
[23] B. Gillot, H. Souha, M. Radid, J. Alloys Compd. 184 (1992) 211.
[24] B. Gillot, M. Radid, K. Sbai, H. Souha, J. Alloys Compd. 274 (1998) 90.
[25] N. Saunders, Calphad 9 (1985) 297.
[26] http://www.asminternational.org/AsmEnterprise/APD.
[27] User's manual for Lindberg/blue tube furnace TF55035 A-1, Thermo Electron Corporation.
[28] http://en.wikipedia.org/wiki/Titanium_tetrachloride#cite_note-2.
[29] R. Alexandrescu, F. Dumitrache, I. Morjan, I. Sandu, M. Savoiu, I. Voicu, C. Fleaca, R. Piticescu, Nanotechnology 15 (2004) 537–545.
[30] C. Lavoie, M. Meunier, R. Izquierdo, S. Boivin, P. Desjardins, Appl. Phys. A 53 (1991) 339.
[31] http://en.wikipedia.org/wiki/Titanium_tetrachloride.
[32] M. Addamo, V. Augugliaro, A.D. Paola, E. Garcıa-Lopez, V. Loddo, G. Marcı, L. Palmisano, Colloids Surf. A: Physicochem. Eng. Aspects 265 (2005) 23–31.
[33] T. Yu, Y.W. Zhu, X.J. Xu, K.S. Yeong, Z.X. Shen, P. Chen, C.T. Lim, J.T.L. Thong, C.H. Sow, Small 2 (2006) 80.
[34] Z.L. Wang, Adv. Mater. 15 (2003) 432.
[35] J.M. Wu, W.T. Wu, H.C. Shih, J. Electrochem. Soc. 152 (2005) G613.
[36] S. Daothong, N. Songmee, S. Thongtem, P. Singjai, Scr. Mater. 57 (2007) 567.
[37] M. Ouyang, R. Bai, L. Yang, Q. Chen, Y. Han, M. Wang, Y. Yang, H. Chen, J. Phys. Chem. C 112 (2008) 2343.
[38] F. Dachille, P.Y. Simons, R. Roy, Am. Mineral. 53 (1968) 1929.
[39] X.K. Zhao, J.H. Fendler, J. Phys. Chem. 95 (1991) 3716–3723.
[40] P.M. Kumar, S. Badrinarayanan, M. Sastry, Thin Solid Films 358 (2000) 122–130.
[41] M.A. Reddy, M.S. Kishore, V. Pralong, V. Caignaert, U.V. Varadaraju, B. Raveau, Electrochem. Commun. 8 (2006).
[42] F.A. Grant, Rev. Mod. Phys. 31 (1959) 646–674.
[43] E. Kobayashi, T. Wakasugi, G. Mizutani, S. Ushioda, Surf. Sci. 402–404 (1998) 537–541.